KEK Preprint 2000-83
BELLE-CONF-0014
August 2000
H

Measurement of Polarization of J/ψ in $B^0 \to J/\psi + K^{*0}$ and $B^+ \to J/\psi + K^{*+}$ Decays

The Belle Collaboration

Submitted to the XXXth International Conference on High Energy Physics, July-August 2000, Osaka, Japan.

High Energy Accelerator Research Organization (KEK)

KEK Reports are available from:

Information Resources Division
High Energy Accelerator Research Organization (KEK)
1-1 Oho, Tsukuba-shi
Ibaraki-ken, 305-0801
JAPAN

Phone: +81-298-64-5137
Fax: +81-298-64-4604
E-mail: adm-jouhoushiryou1@ccgemail.kek.jp
Internet: http://www.kek.jp

BELLE-CONF-0014
Parallel Session: PA-07
Plenary Session: PL-01b

Measurement of Polarization of J/ψ in $B^0 \to J/\psi + K^{*0}$ and $B^+ \to J/\psi + K^{*+}$ Decays

The Belle Collaboration

Abstract

The polarization of J/ψ is measured in $B^0 \to J/\psi + K^{*0}$ and $B^+ \to J/\psi + K^{*+}$ decays. A data sample corresponding to an integrated luminosity of 5.1 fb^{-1} has been collected by the Belle detector at the KEKB electron-positron collider and used for the analysis. The polarization is determined from the angular distribution of the decay of J/ψ and K^*. Preliminary results of the polarization measurement and the transversity analysis are presented.

Typeset using REVTEX

A. Abashian[44], K. Abe[8], K. Abe[36], I. Adachi[8], Byoung Sup Ahn[14], H. Aihara[37], M. Akatsu[19], G. Alimonti[7], K. Aoki[8], K. Asai[20], M. Asai[9], Y. Asano[42], T. Aso[41], V. Aulchenko[2], T. Aushev[12], A. M. Bakich[33], E. Banas[15], S. Behari[8], P. K. Behera[43], D. Beiline[2], A. Bondar[2], A. Bozek[15], T. E. Browder[7], B. C. K. Casey[7], P. Chang[23], Y. Chao[23], B. G. Cheon[32], S.-K. Choi[6], Y. Choi[32], Y. Doi[8], J. Dragic[17], A. Drutskoy[12], S. Eidelman[2], Y. Enari[19], R. Enomoto[8,10], C. W. Everton[17], F. Fang[7], H. Fujii[8], K. Fujimoto[19], Y. Fujita[8], C. Fukunaga[39], M. Fukushima[10], A. Garmash[2,8], A. Gordon[17], K. Gotow[44], H. Guler[7], R. Guo[21], J. Haba[8], T. Haji[4], H. Hamasaki[8], K. Hanagaki[29], F. Handa[36], K. Hara[27], T. Hara[27], T. Haruyama[8], N. C. Hastings[17], K. Hayashi[8], H. Hayashii[20], M. Hazumi[27], E. M. Heenan[17], Y. Higashi[8], Y. Higasino[19], I. Higuchi[36], T. *Higuchi*[37], T. *Hirai*[38], *H. Hirano*[40], *M. Hirose*[19], T. *Hojo*[27], Y. *Hoshi*[35], K. *Hoshina*[40], W.-S. Hou[23], S.-C. Hsu[23], H.-C. Huang[23], Y.-C. Huang[21], S. Ichizawa[38], Y. Igarashi[8], T. Iijima[8], H. Ikeda[8], K. Ikeda[20], K. Inami[19], Y. Inoue[26], A. Ishikawa[19], R. Itoh[8], G. Iwai[25], M. Iwai[8], H. Iwasaki[8], Y. Iwasaki[8], D. J. Jackson[27], P. Jalocha[15], H. K. Jang[31], M. Jones[7], R. Kagan[12], H. Kakuno[38], J. Kaneko[38], J. H. Kang[45], J. S. Kang[14], P. Kapusta[15], K. Kasami[8], N. Katayama[8], H. Kawai[3], M. Kawai[8], N. Kawamura[1], T. Kawasaki[25], H. Kichimi[8], D. W. Kim[32], Heejong Kim[45], H. J. Kim[45], Hyunwoo Kim[14], S. K. Kim[31], K. Kinoshita[5], S. Kobayashi[30], S. Koike[8], Y. Kondo[8], H. Konishi[40], K. Korotushenko[29], P. Krokovny[2], R. Kulasiri[5], S. Kumar[28], T. Kuniya[30], E. Kurihara[3], A. Kuzmin[2], Y.-J. Kwon[45], M. H. Lee[8], S. H. Lee[31], C. Leonidopoulos[29], H.-B. Li[11], R.-S. Lu[23], Y. Makida[8], A. Manabe[8], D. Marlow[29], T. Matsubara[37], T. Matsuda[8], S. Matsui[19], S. Matsumoto[4], T. Matsumoto[19], K. Misono[19], K. Miyabayashi[20], H. Miyake[27], H. Miyata[25], L. C. Moffitt[17], G. R. Moloney[17], G. F. Moorhead[17], N. Morgan[44], S. Mori[42], T. Mori[4], A. Murakami[30], T. Nagamine[36], Y. Nagasaka[18], Y. Nagashima[27], T. Nakadaira[37], T. Nakamura[38], E. Nakano[26], M. Nakao[8], H. Nakazawa[4], J. W. Nam[32], S. Narita[36], Z. Natkaniec[15], K. Neichi[35], S. Nishida[16], O. Nitoh[40], S. *Noguchi*[20], T. *Nozaki*[8], S. *Ogawa*[34], R. *Ohkubo*[8], T. *Ohshima*[19], Y. *Ohshima*[38], T. Okabe[19], T. Okazaki[20], S. Okuno[13], S. L. Olsen[7], W. Ostrowicz[15], H. Ozaki[8], P. Pakhlov[12], H. Palka[15], C. S. Park[31], C. W. Park[14], H. Park[14], L. S. Peak[33], M. Peters[7], L. E. Piilonen[44], E. Prebys[29], J. Raaf[5], J. L. Rodriguez[7], N. Root[2], M. Rozanska[15], K. Rybicki[15], J. Ryuko[27], H. Sagawa[8], Y. Sakai[8], H. Sakamoto[16], H. Sakaue[26], M. *Satapathy*[43], N. *Sato*[8], A. *Satpathy*[8,5], S. *Schrenk*[44], S. *Semenov*[12], Y. *Settai*[4], M. E. Sevior[17], H. Shibuya[34], B. Shwartz[2], A. Sidorov[2], V. Sidorov[2], S. Stanič[42], A. Sugi[19], A. Sugiyama[19], K. Sumisawa[27], T. Sumiyoshi[8], J. Suzuki[8], J.-I. Suzuki[8], K. Suzuki[3], S. Suzuki[19], S. Y. Suzuki[8], S. K. Swain[7], H. Tajima[37], T. Takahashi[26], F. Takasaki[8], M. Takita[27], K. Tamai[8], N. Tamura[25], J. Tanaka[37], M. Tanaka[8], Y. Tanaka[18], G. N. Taylor[17], Y. Teramoto[26], M. Tomoto[19], T. Tomura[37], S. N. Tovey[17], K. Trabelsi[7], T. Tsuboyama[8], Y. Tsujita[42], T. Tsukamoto[8], T. Tsukamoto[30], S. Uehara[8], K. Ueno[23], N. Ujiie[8], Y. Unno[3], S. Uno[8], Y. Ushiroda[16], Y. Usov[2], S. E. Vahsen[29], G. Varner[7], K. E. Varvell[33], C. C. Wang[23], C. H. Wang[22], M.-Z. Wang[23], T.-J. Wang[11], Y. Watanabe[38], E. Won[31], B. D. Yabsley[8], Y. Yamada[8], M. Yamaga[36], A. Yamaguchi[36], H. Yamaguchi[8], H. Yamamoto[7], H. Yamaoka[8], Y. Yamaoka[8], Y. Yamashita[24], M. Yamauchi[8], S. Yanaka[38], M. *Yokoyama*[37], K. *Yoshida*[19], Y. Yusa[36], H. Yuta[1], C.-C. Zhang[11], H. W. Zhao[8], Y. Zheng[7], V. Zhilich[2], and D. Žontar[42]

[1]Aomori University, Aomori

[2]Budker Institute of Nuclear Physics, Novosibirsk
[3]Chiba University, Chiba
[4]Chuo University, Tokyo
[5]University of Cincinnati, Cincinnati, OH
[6]Gyeongsang National University, Chinju
[7]University of Hawaii, Honolulu HI
[8]High Energy Accelerator Research Organization (KEK), Tsukuba
[9]Hiroshima Institute of Technology, Hiroshima
[10]Institute for Cosmic Ray Research, University of Tokyo, Tokyo
[11]Institute of High Energy Physics, Chinese Academy of Sciences, Beijing
[12]Institute for Theoretical and Experimental Physics, Moscow
[13]Kanagawa University, Yokohama
[14]Korea University, Seoul
[15]H. Niewodniczanski Institute of Nuclear Physics, Krakow
[16]Kyoto University, Kyoto
[17]University of Melbourne, Victoria
[18]Nagasaki Institute of Applied Science, Nagasaki
[19]Nagoya University, Nagoya
[20]Nara Women's University, Nara
[21]National Kaohsiung Normal University, Kaohsiung
[22]National Lien-Ho Institute of Technology, Miao Li
[23]National Taiwan University, Taipei
[24]Nihon Dental College, Niigata
[25]Niigata University, Niigata
[26]Osaka City University, Osaka
[27]Osaka University, Osaka
[28]Panjab University, Chandigarh
[29]Princeton University, Princeton NJ
[30]Saga University, Saga
[31]Seoul National University, Seoul
[32]Sungkyunkwan University, Suwon
[33]University of Sydney, Sydney NSW
[34]Toho University, Funabashi
[35]Tohoku Gakuin University, Tagajo
[36]Tohoku University, Sendai
[37]University of Tokyo, Tokyo
[38]Tokyo Institute of Technology, Tokyo
[39]Tokyo Metropolitan University, Tokyo
[40]Tokyo University of Agriculture and Technology, Tokyo
[41]Toyama National College of Maritime Technology, Toyama
[42]University of Tsukuba, Tsukuba
[43]Utkal University, Bhubaneswer
[44]Virginia Polytechnic Institute and State University, Blacksburg VA
[45]Yonsei University, Seoul

I. INTRODUCTION

The measurement of the polarization of J/ψ in the decay $B \to J/\psi + K^*$ is a good test of the factorization hypothesis [1]. In addition, this decay mode plays an important role in the study of the CP violation since the decay $B^0 \to J/\psi K^{*0} \to J/\psi K_S \pi^0$ is a CP specific state. However, since the $J/\psi K^*$ system has three different possible helicity states, CP even and odd states are mixed. The measurement of the polarization of J/ψ gives information on the amount of the mixing.

The polarization can be studied in two different bases. One is the helicity basis and the other is the transversity basis. The former is the conventional method and is used to measure the longitudinal polarization of J/ψ. Previous measurements of this value widely fluctuate as summarized in Table I. Earlier measurements by ARGUS [2] and CLEO II [3] show very high values close to 1, which is inconsistent with predictions from most of the factorization models [4]. This inconsistency raised a broad argument among theorists. CDF [5] then measured the polarization and obtained a lower value which is consistent with the models, as did the re-measurement by CLEO II [6]. The aim of this paper is to measure this value with better precision using higher statistics.

The longitudinal polarization represents the amount of the helicity $|0,0>$ component which is a pure CP even eigenstate in $B^0 \to J/\psi K^{*0} \to J/\psi K_S \pi^0$. However, the remaining helicity states $|\pm 1, \pm 1>$ are CP mixed states and their CP eigenstate composition cannot be determined from the longitudinal polarization. The transversity basis analysis [7] projects out CP components from such CP mixed states by measuring the transverse parity polarization. The measurement of the polarization is useful for future CP asymmetry measurement using this decay mode.

In this paper, we present measurements of both longitudinal and transverse parity polarizations of the J/ψ in $B \to J/\psi K^*$ decays. The measurements are performed using a sophisticated fit based on an unbinned likelihood method.

Experiment	Γ_L/Γ
ARGUS (1994)	$0.97 \pm 0.16 \pm 0.15$
CLEO II (1994)	$0.80 \pm 0.08 \pm 0.05$
CDF (1995)	$0.65 \pm 0.10 \pm 0.04$
CLEO II (1996)	$0.52 \pm 0.07 \pm 0.04$

TABLE I. Previous measurement of Γ_L/Γ.

II. DATA SAMPLE

The polarization of the J/ψ was measured by reconstructing both neutral and charged B meson decays into the following 3 final states:

1. $B^0 \to J/\psi K^{*0}$ $(K^{*0} \to K^+\pi^-)$,
2. $B^+ \to J/\psi K^{*+}$ $(K^{*+} \to K_S\pi^+)$,

3. $B^+ \to J/\psi K^{*+}$ ($K^{*+} \to K^+\pi^0$),

and their charge conjugates.

The data sample used in this analysis corresponds to an integrated luminosity of 5.1 fb^{-1} acquired by the Belle detector [8] at the KEKB electron-positron collider [9]. Events which pass the hadronic event selection and satisfy $R_2 < 0.5$ are used in the analysis, where R_2 is the ratio of the second to 0'th Fox-Wolfram parameter. Candidate $B \to J/\psi K^*$ decays are reconstructed in the following steps.

A. Reconstruction of J/ψ

The reconstruction of the J/ψ is performed using dilepton decays, i.e. $J/\psi \to e^+e^-$ and $\mu^+\mu^-$. For e^+e^- decays, electrons and positrons are identified by combining information from several detectors such as the matching between the energy measured in the calorimeter (ECL) and the momentum measured in the central drift chamber (CDC), the shower shape of the cluster energy deposit in ECL, dE/dx measured in the CDC. A likelihood is calculated from these measurements and it is required to be consistent with electrons. If there is an energy cluster in the calorimeter within 0.05 radians of the identified track, its energy is added to that of the track. This is done to include photons emitted by radiative decay of J/ψ. The invariant mass of two tracks, both of which satisfy the criteria above and have the opposite charges, is calculated and the tracks are identified as a $J/\psi \to e^+e^-$ if the mass is in the range 2.8 GeV/c^2 $< M(e^+e^-) <$ 3.2 GeV/c^2.

Muons are identified by looking at the tracks which have associated hits in the muon detector (KLM). The number of hit layers in the KLM is compared with the expected number calculated from the momentum measured in the CDC and the muon likelihood is calculated combined with the energy deposit information of the associated ECL hit. A track whose likelihood is high is identified as a muon track. The dimuon invariant mass is required to be in the range 3.0 GeV/c^2 $< M(\mu^+\mu^-) <$ 3.16 GeV/c^2 to be identified as a J/ψ.

For the identified lepton tracks, a kinematic fit with a vertex and mass constraint is performed to improve the mass resolution.

B. Reconstruction of K^{*0} and K^{*+}

The K^{*0} and K^{*+} candidates are reconstructed by looking at the decay modes $K^{*0} \to K^+\pi^-$, $K^{*\pm} \to K_S\pi^\pm$ and $K^{*\pm} \to K^\pm\pi^0$ and their charge conjugates. In the reconstruction, charged kaons are identified by requiring the kaon likelihood of a track is high. The kaon likelihood is obtained by combining measurements of the time of flight by scintillation counters (TOF), dE/dx by the CDC and hit information in the aerogel Cerenkov counters (ACC). The tracks which are not identified as kaons nor leptons in the J/ψ reconstruction are treated as charged pion candidates.

The K_S candidates are reconstructed from two oppositely-charged pions which satisfy the following conditions: 1) the closest distance of both pion tracks to each other is less than 0.03 cm, 2) the opening angle between them is less than 0.15 radians, and 3) the reconstructed decay vertex of K_S is at least 0.1 cm from the interaction point. The invariant mass is calculated and a pion pair with 0.47 GeV/c^2 $< M(\pi^+\pi^-) <$ 0.52 GeV/c^2 is identified as a K_S. A vertex constraint fit is performed for the pion pair to improve the mass resolution. The π^0 reconstruction is performed by searching for two clusters in the ECL with energy greater than 40 MeV. A photon pair with invariant mass in the range 0.125 GeV/c^2 $< M(\gamma\gamma) <$ 0.145 GeV/c^2 is identified as a π^0. A mass constraint fit is performed to obtain the momentum of the π^0.

A K^{*0} is identified if the difference of the invariant mass of an identified kaon-pion pair is within 75 MeV/c^2 of the nominal K^* mass.

C. Reconstruction of B^0 and B^+

The B^0 and B^+ reconstruction is performed by calculating the beam constrained mass (M_{bc}) and the energy difference between the B candidate and the beam energy (ΔE). The scatter plot of M_{bc} and ΔE is shown in Figs 1 - 3 for each of $J/\psi K^{*0}(K^{*0} \to K^+\pi^-)$, $J/\psi K^{*+}(K^{*+} \to K_S\pi^+)$, and $J/\psi K^{*+}(K^{*+} \to K^+\pi^0)$ decay modes, together with the projection onto each axis. The signal region is determined so that the width of the region covers 3σ from the peak. The beam constrained mass is required to be between 5.27 and 5.29 GeV/c^2. $|\Delta E|$ is required to be less than 30 MeV for $J/\psi K^{*0}(K^{*0} \to K^+\pi^-)$ and $J/\psi K^{*+}(K^{*+} \to K_S\pi^+)$, while it is required to be less than 45 MeV for $J/\psi K^{*+}(K^{*+} \to K^+\pi^0)$ because of shower leakage in the π^0 reconstruction. When an event has multiple entries in the signal region, the combination whose M_{bc} and ΔE values are the closest to $M_{bc} = 5.279$ GeV/c^2 and $\Delta E = 0.0$ GeV in the $M_{bc} - \Delta E$ plane is taken.

Decay Mode		Yield	Efficiency(%)
$B^0 \to J/\psi(K^+\pi^-)^{*0}$	$J/\psi \to e^+e^-$	49	20.9
	$J/\psi \to \mu^+\mu^-$	62	23.3
$B^+ \to J/\psi(K_S\pi^+)^{*+}$	$J/\psi \to e^+e^-$	18	13.3
	$J/\psi \to \mu^+\mu^-$	13	15.8
$B^+ \to J/\psi(K^+\pi^0)^{*+}$	$J/\psi \to e^+e^-$	12	10.3
	$J/\psi \to \mu^+\mu^-$	22	12.6

TABLE II. Signal yields in the data sample and the efficiency estimated by Monte Carlo.

In $J/\psi K^{*+}(K^{*+} \to K^+\pi^0)$ reconstruction, the angle of the kaon with respect to the K^* direction in the K^* rest frame ($\cos\theta_{K^*}$) is required to satisfy $\cos\theta_{K^*} < 0.8$ to eliminate slow pion backgrounds. This is equivalent to a constraint on the π^0 minimum momentum of about 200 MeV/c in the CM frame. The numbers of reconstructed events that pass these selection criteria are summarized in Table II.

The detection efficiency for each decay mode is estimated by applying the same selection criteria to Monte Carlo event samples. The estimated efficiencies are given in Table II. Monte Carlo events are generated assuming a flat angular distribution using the QQ event generator [10]. The generated events are passed through a detector simulation program based on GEANT3 [12] and then are fed into the same reconstruction chain as that used for data.

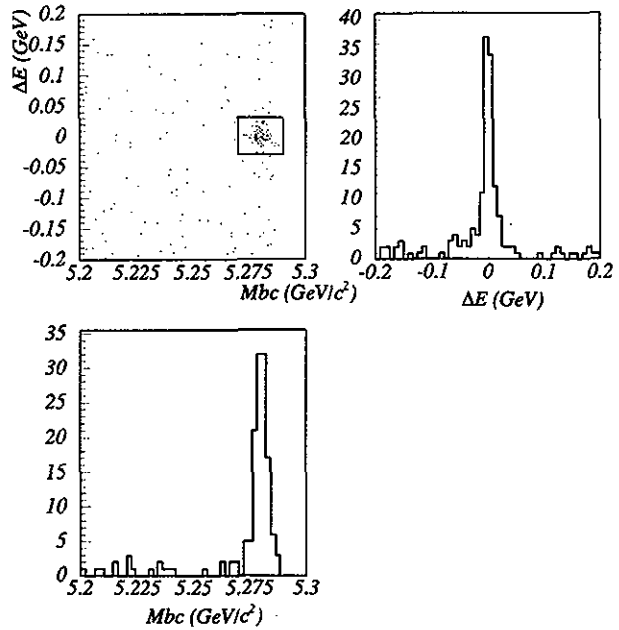

FIG. 1. Scatter plot of ΔE vs. M_{bc} for $B^0 \to J/\psi K^{*0}(K^{*0} \to K^+\pi^-)$. The signal region is shown in the box. The projections onto ΔE and M_{bc} are also shown.

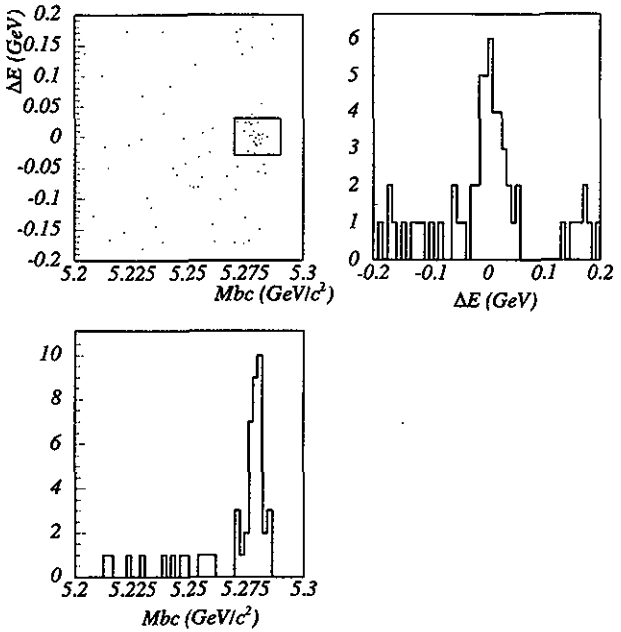

FIG. 2. Scatter plot of ΔE vs. M_{bc} for $B^+ \to J/\psi K^{*+}(K^{*+} \to K_S\pi^+)$. The signal region is shown in the box. The projections onto ΔE and M_{bc} are also shown.

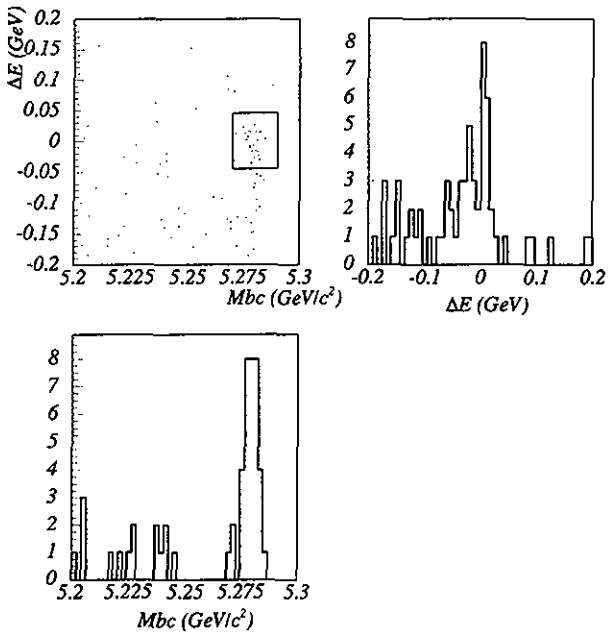

FIG. 3. Scatter plot of ΔE vs. M_{bc} for $B^+ \to J/\psi K^{*+}(K^{*+} \to K^+\pi^0)$. The signal region is shown in the box. The projections onto ΔE and M_{bc} are also shown.

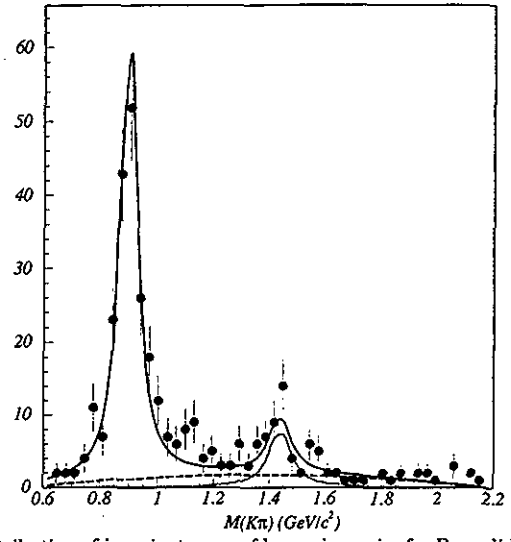

FIG. 4. The distribution of invariant mass of kaon-pion pairs for B candidates without the K^* mass window selection. The solid line shows the fit to two Breit-Wigner functions corresponding to $K^*(892)$ and $K_2^*(1430)$ with a background function. The dotted line shows the $K_2^*(1430)$ component while the background component in the dashed line.

D. Background Estimation

The contamination of background in the selected event sample is studied for several sources.

The first source is the feed across from one $B \to J/\psi K^*$ mode to another. This can be one of the major background sources since the total energy and the beam constrained mass are similar. The amount of feed across among the six major J/ψ exclusive decay modes is estimated using Monte Carlo.

The second source is from non-resonant production such as $B \to J/\psi K\pi$. The contamination from non-resonant decay is studied by looking at the events in the K^* mass sideband. Fig. 4 shows the $K\pi$ mass distribution for events selected by the criteria used for the signal reconstruction without requiring the K^* mass window. As reported by CLEO [6], some excess is observed in the high mass region of 1.1 to 1.6 GeV/c^2. In particular, there appears to be a peak near 1.43 GeV/c^2. We assume the peak is from $B \to J/\psi K_2^*(1430)$ decay and fit the $K\pi$ mass distribution with two Breit-Wigner functions describing the $K^*(892)$ and $K_2^*(1430)$ mass peaks combined with a second order polynomial as a background function. The peak position and width in the Breit-Wigner functions are fixed at PDG values in the fit. The contamination of the non-resonant decay background is estimated from the fitted functions.

The third source is the contamination from other B decays. This category consists of contamination from other J/ψ inclusive decays, feed down from higher charmonium states to

J/ψ, and combinatorial background events. These backgrounds are evaluated using Monte Carlo.

The last source is contamination from continuum events. This is also estimated by Monte Carlo with the LUND73 event generator [11].

The results of the estimation are summarized in Table III. The numbers show the fraction of each background source in the event sample. As seen, the overall contamination of background is less than ~12%. The largest background comes from non-resonant $K\pi$ production which is about 4%. The contamination from the possible $K_2^*(1430)$ tail is negligible. However, the high mass excess in the K^* sideband is still not well understood and this estimation is not reliable. In this analysis, a systematic error of 100% is assigned to this value. The contamination of the feed across is different in each reconstructed mode, varying from 1 to 7 %. The background from other B decays is very small. For continuum background, no events remained after applying the same selection to 10 million continuum events generated by the Monte Carlo in all three modes. Therefore background contamination from continuum events is omitted in the analysis.

The overall background contamination is cross checked by comparing the estimated backgrounds with the events in the ΔE and M_{bc} sidebands. It is consistent.

		$J/\psi(K^+\pi^-)^{*0}$	$J/\psi(K_S\pi^+)^{*+}$	$J/\psi(K^+\pi^0)^{*+}$
Signal(r_{sig})		94.1	89.2	88.2
Feed Across (r^i_{fa})	$J/\psi(K^+\pi^-)^{*0}$	-	3.3	7.1
	$J/\psi(K_S\pi^+)^{*+}$	0.2	-	<0.1
	$J/\psi(K^+\pi^0)^{*+}$	0.9	<0.1	-
	$J/\psi(K_S\pi^0)^{*0}$	0.1	2.8	0.1
	$J/\psi K^+$	<0.1	<0.1	<0.1
	$J/\psi K_S$	0.3	<0.1	0.1
Non resonant (r_{nr})		4.1	4.1	4.1
Other B decays (r_{combi})		0.1	0.2	0.1
Continuum		<0.1	<0.1	<0.1

TABLE III. The percentage of signal and individual background components for each channel.

III. MEASUREMENT OF LONGITUDINAL POLARIZATION

The longitudinal polarization of the J/ψ is measured using the helicity basis. Fig. 5 shows the definition of angles used in the analysis. The decay angle θ_ψ is the angle of the positive lepton with respect to the moving direction of the J/ψ defined in the J/ψ rest frame. The angle θ_{K^*} is defined similarly for the kaon from the K^*.

The decay angles θ_ψ and θ_{K^*} are related to the longitudinal polarization Γ_L/Γ of J/ψ as [6] [13]:

$$\frac{1}{\Gamma}\frac{d^2\Gamma}{d\cos\theta_\psi d\cos\theta_{K^*}} = \frac{9}{32}(1+\cos^2\theta_\psi)\sin^2\theta_{K^*}(1-\frac{\Gamma_L}{\Gamma}) + \frac{9}{8}\sin^2\theta_\psi\cos^2\theta_{K^*}\frac{\Gamma_L}{\Gamma} \quad (1)$$

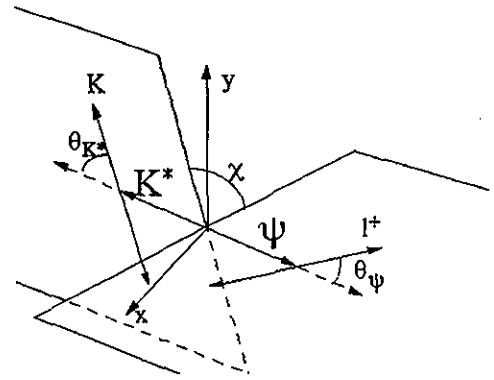

FIG. 5. The definition of angle used in the helicity analysis

The polarization of the J/ψ in $B \to J/\psi K^*$ decays is obtained by fitting this formula to the measured 2-dimensional distribution of $\cos\theta_\psi$ and $\cos\theta_{K^*}$, taking the detection efficiency and the effect of the backgrounds into account.

The fit is performed using an unbinned likelihood method. The probability density function (PDF) is defined using the theoretical distribution in (1) and can be expressed as

$$\begin{aligned} PDF(x,y) = r_{sig} \times \epsilon(x,y) \cdot \frac{1}{\Gamma}\frac{d^2\Gamma}{dxdy}(x,y) \\ + \sum_{feedacross} r^i_{fa} \times \epsilon^i_{fa}(x,y) \cdot f^i_{fa} \\ + r_{nr} \times f_{nr}(x,y) \\ + r_{combi} \times f_{combi} \end{aligned} \quad (2)$$

where $x = \cos\theta_\psi$ and $y = \cos\theta_{K^*}$. $\epsilon(x,y)$ is the detector efficiency as a function of two angles. $\epsilon^i_{fa}(x,y)$ is the efficiency for i'th feed across mode as a function of two angles. The i runs over all the feed across modes listed in Table III. f^i_{fa}, $f_{nr}(x,y)$ and f_{combi} are the angular shapes for i'th feed across mode, the non resonant contribution and the combinatorial background, respectively.

r_{sig}, r^i_{fa}, r_{nr}, r_{combi} are fractions of signal events, i'th feed across contamination, non-resonant contamination and combinatorial background in the event sample, respectively. These are obtained by the efficiency and background study described in the previous sections. The numbers listed in Table III are used.

The detector efficiency functions $\epsilon(x,y)$ and $\epsilon(x,y)^i_{fa}$ are obtained using a large Monte Carlo data sample (200000 events in total) generated with a flat angular distribution. The events are histogrammed in a 10×10 mesh in the $\cos\theta_\psi - \cos\theta_{K^*}$ plane and the distribution is fitted with a 2 dimensional polynomial. The efficiency functions are almost flat except for the large $\cos\theta_{K^*}$ region where slow pions dominate.

The angular shape for the non-resonant decay $f_{nr}(x,y)$ is estimated by using Monte Carlo events generated assuming phase space decay. The effect of the detector efficiency

is included in this function. The events are histogrammed in a similar way used to obtain efficiency functions and are fitted with a 2 dimensional polynomial. The angular distribution for the feed across and the combinatorial backgrounds is assumed to be flat.

We perform a fit to the angular distribution obtained for three decay modes separately where the longitudinal polarization is the only free parameter. We also perform a simultaneous fit to all of three modes by defining a single likelihood. In this case, the probability density function is obtained by taking the weighted sum of the PDF for each mode. The weighting factor is derived from the observed number of events.

Fig. 6 shows the distribution in the $\cos\theta_\psi - \cos\theta_{K^*}$ plane for reconstructed $B^0 \to J/\psi K^{*0}(K^{*0} \to K^+\pi^-)$ together with the fitted PDF shape. The shape of the theoretical distribution in (1) with the measured longitudinal polarization is also shown. Fig. 7 shows the shapes of the distribution projected onto $\cos\theta_\psi$ and $\cos\theta_{K^*}$ for the combined distribution of three reconstructed modes. The distributions are background-subtracted and efficiency-corrected. The projected shapes of the theoretical function (1) with the measured longitudinal polarization are shown in solid lines. As seen, the function reproduces the measured distributions reasonably well. The longitudinal polarization values of the J/ψ (Γ_L/Γ) obtained from fits are summarized in Table IV. The results are preliminary.

Mode	Γ_L/Γ
$J/\psi(K^+\pi^-)^{*0}$	0.56 ± 0.07
$J/\psi(K_S\pi^+)^{*+}$	0.39 ± 0.16
$J/\psi(K^+\pi^0)^{*+}$	0.48 ± 0.18
Global fit	0.52 ± 0.06

TABLE IV. Longitudinal polarization of J/ψ (Γ_L/Γ) obtained from fits.

IV. MEASUREMENT OF TRANSVERSE PARITY POLARIZATION

Fig. 8 shows the angle definition in the transversity analysis. The transversity axis is defined as an axis perpendicular to the K^* decay plane spanned in the J/ψ rest frame. The θ_{tr} is the angle of a positive lepton from J/ψ decay with respect to the transversity axis.

The distribution of $\cos\theta_{tr}$ can be expressed as a function of the transverse parity polarization $A_\perp$ in [6] [7]

$$\frac{1}{\Gamma}\frac{d\Gamma}{d\cos\theta_{tr}} = \frac{3}{8}(1+\cos^2\theta_{tr})(1-|A_\perp|^2) + \frac{3}{4}|A_\perp|^2\sin^2\theta_{tr} \qquad (3)$$

The procedure of the fit is the same as that used for the longitudinal polarization measurement. The probability density function is formed in a similar way. The transverse parity polarization is measured by a single parameter fit to the angular distributions of $\cos\theta_{tr}$ for the reconstructed modes.

Fig. 9 shows the combined distribution of $\cos\theta_{tr}$ for all reconstructed modes. The distribution is background-subtracted and efficiency-corrected. The function shape of (3) with the obtained polarization is shown as a solid line. The distribution is reproduced by the function reasonably well. The results of the fits are summarized in Table V. The values are preliminary.

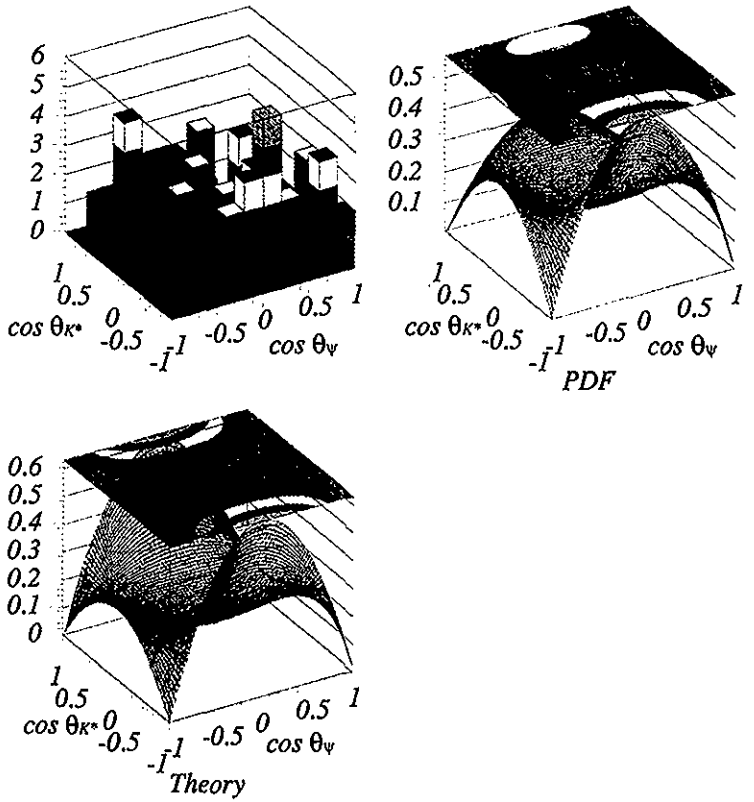

FIG. 6. The distribution of data in $\cos\theta_\psi$ and $\cos\theta_K^*$ for reconstructed $J/\psi K^{*0}(K^{*0} \to K^+\pi^-)$. The fitted PDF shape is also shown in the upper right. The lower figure shows the shape of theoretical angular distribution (1) with the measured longitudinal polarization for this mode.

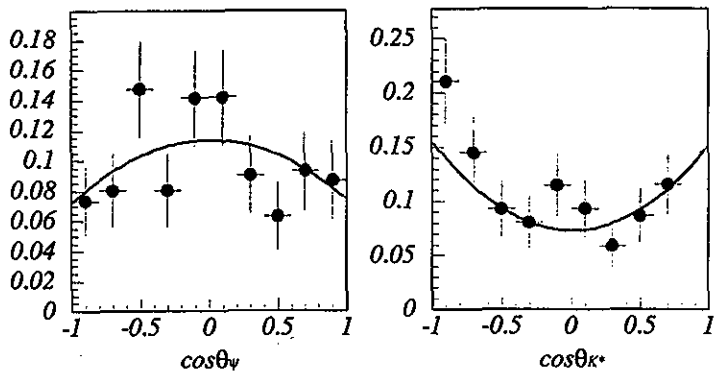

FIG. 7. The projections onto $\cos\theta_\psi$ and $\cos\theta_{K^*}$. The distributions for all of three reconstructed $B \to J/\psi K^*$ modes are combined. The distributions are background-subtracted and corrected for the detector acceptance. Solid lines show the fit results.

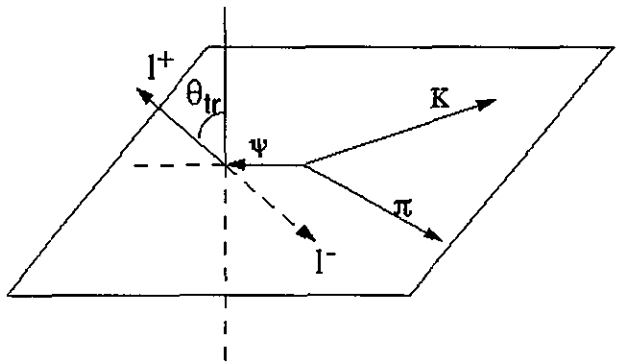

FIG. 8. The definition of angles used in the transversity analysis

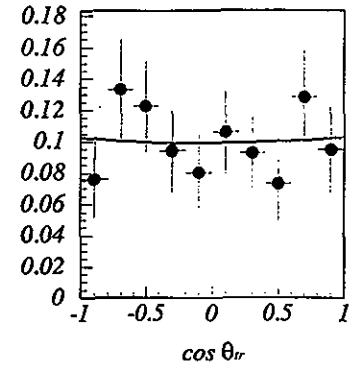

FIG. 9. The combined distribution of $\cos\theta_{tr}$ for three reconstructed $B \to J/\psi K^*$ modes. The distribution is background-subtracted and acceptance-corrected. The solid line shows the fit result.

Mode	$\lvert A_\perp\rvert^2$
$J/\psi(K^+\pi^-)^{*0}$	0.27 ± 0.13
$J/\psi(K_S\pi^+)^{*+}$	0.07 ± 0.32
$J/\psi(K^+\pi^0)^{*+}$	0.49 ± 0.26
Global fit	0.27 ± 0.11

TABLE V. Transverse parity polarization ($|A_\perp|^2$) obtained from fits.

V. ESTIMATION OF SYSTEMATIC UNCERTAINTIES

Uncertainties in the following items are considered as the sources of the systematic uncertainty in the polarization measurement:

1. the efficiency function parameterization,
2. the ratio factors and the angular shape of feed across modes,
3. the ratio factor and the angular shape of non-resonant decays, and
4. the ratio factor and the angular shape of combinatorial backgrounds.

The uncertainty in the efficiency function parameterization is limited by the Monte Carlo statistics and the goodness of the parameterization fit. To estimate the uncertainty, the measured polarization value is compared with the result obtained without using the efficiency function in the PDF.

The normalization of the non-resonant contamination r_{nr} has a large ambiguity as described in the previous section and the uncertainty of 100% is assigned to r_{nr}. As for the angular distribution of non-resonant contamination which is assumed to follow the phase

space decay, there may be a polarization effect in the distribution. The ambiguity is estimated by studying the difference from the case with the polarized angular distribution where the polarization is set at the measured value.

The ratio factors of the feed across backgrounds r_{fa} and of the combinatorial background r_{combi} are estimated using the Monte Carlo events and their uncertainties mainly come from the limited statistics. So we conservatively assign 100% error in r_{fa} and r_{combi}.

The angular shape for the feed across modes and the combinatorial background is assumed to be flat in the fit, however, there may be a possible polarization effect also. This uncertainty is estimated in a similar way as that used for the non-resonant contamination.

The results of the systematic error analyses are summarized in Table VI. We take the linear sum of these values as the systematic uncertainty in the measured values.

	Γ_L/Γ	$\lvert A_\perp\rvert^2$
Efficiency function	0.010	0.012
Ratio of feed across	0.006	0.005
Polarization in feed across	0.010	0.010
Ratio of non-resonant	0.007	0.005
Polarization in non-resonant	0.010	0.015
Ratio of combinatorial background	<0.001	<0.001
Polarization effect in combinatorial background	<0.001	<0.001
sum	0.043	0.047

TABLE VI. Table of systematic uncertainties in the polarization measurements.

VI. CONCLUSION

We have measured the longitudinal polarization and the transverse parity polarization of the J/ψ in $B^0 \to J/\psi + K^{*0}$ and $B^+ \to J/\psi + K^{*+}$ decays from the angular distribution of the J/ψ and K^* decays. The measurement is done by an unbinned likelihood fit to the angular distribution of decay products obtained for the selected event sample of 176 events in total. The probability density function is formed by considering the effect of the detector efficiency and the background contamination. We obtained the following preliminary results from the fits:

$$\Gamma_L/\Gamma = 0.52 \pm 0.06 \pm 0.04, \text{ and}$$
$$|A_\perp|^2 = 0.27 \pm 0.11 \pm 0.05.$$

The measured values are consistent with the measurements by CDF [5] and CLEO II [6] (2nd measurement). The value of the transverse parity polarization indicates that the CP even state dominates in the $B^0 \to J/\psi K^{*0}(K^{*0} \to K_S\pi^0)$ decay.

ACKNOWLEDGMENTS

We gratefully acknowledge the efforts of the KEKB group in providing us with excellent luminosity and running conditions and the help with our computing and network systems provided by members of the KEK computing research center. We thank the staffs of KEK and collaborating institutions for their contributions to this work, and acknowledge support from the Ministry of Education, Science, Sports and Culture of Japan and the Japan Society for the Promotion of Science; the Australian Research Council and the Australian Department of Industry, Science and Resources; the Department of Science and Technology of India; the BK21 program of the Ministry of Education of Korea and the Basic Science program of the Korea Science and Engineering Foundation; the Polish State Committee for Scientific Research under contract No.2P03B 17017; the Ministry of Science and Technology of Russian Federation; the National Science Council and the Ministry of Education of Taiwan; the Japan-Taiwan Cooperative Program of the Interchange Association; and the U.S. Department of Energy.

REFERENCES

[1] M.Bauer, B.Stech, and M.Wirbel, Z.Phys. C **34**, 103 (1987); M.Wirbel, B.Stech, and M.Bauer, Z.Phys. C **29**, 637 (1985)

[2] H.Albrecht et al. (ARGUS Collaboration), Phys. Lett. B **340**, 217 (1994)

[3] M.S.Alam et al. (CLEO Collaboration), Phys. Rev. D **50**, 43 (1994)

[4] M.Gourdin, A.N.Kamel, and X.Y.Pham, Phys. Rev. Lett. **73**, 3355, (1994); R.Aleksan et al., Phys. Rev. D **51**, 6235, (1995)

[5] F.Abe et al. (CDF Collaboration), Phys. Rev. Lett. **75**, 3068 (1995)

[6] C.S.Jessop et al. (CLEO Collaboration), Phys. Rev. Lett. **79**, 4533 (1997); CLEO Collaboration, CLEO CONF 96-24 (1996)

[7] I.Dunietz, H.Quinn, A.Snyder, W.Toki and H. J.Lipkin, Phys. Rev. D **43**, 2193 (1991).

[8] Belle Collaboration, Technical Design Report, KEK-Report95-1 (1995)

[9] KEKB B-Factory Design Report, KEK-Report95-7 (1995)

[10] See http://www.lns.cornell.edu/public/CLEO/soft/QQ/

[11] T.Sjöstrand, Comp. Phys. Comm. **82**, 74 (1994); T.Sjöstrand and M.Bengtsson, Comp. Phys, Comm., **43**, 367 (1987); T.Sjöstrand, Comp. Phys. Comm. **39**, 347 (1986)

[12] CERN Program Library Long Writeups Q123, GEANT Detector Description and Simulation Tool, see http://wwwinfo.cern.ch/asdoc/geantold/GEANTMAIN.html

[13] G.Kramer and W.F.Palmer, Phys. Rev. D **46**, 2969 (1992)